Published in final edited form as:
Vision Res. 2006 October ; 46(21): 3723–3740.

Short-latency disparity vergence eye movements: A response to disparity energy

B. M. Sheliga, **E. J. FitzGibbon**, and **F. A. Miles**
Laboratory of Sensorimotor Research, National Eye Institute, National Institutes of Health, Bethesda, MD 20892

Abstract

Vergence eye movements were elicited in human subjects by applying disparities to square-wave gratings lacking the fundamental ("missing fundamental", *mf*). Using a dichoptic arrangement, subjects viewed gratings that were identical at the two eyes except for a phase difference of ¼ wavelength so that, based on the nearest-neighbor matches, the features and the 4*n*+1 harmonics (5th, 9th etc) all had binocular disparities of one sign, whereas the 4*n*−1 harmonics (3rd, 7th etc) all had disparities of the opposite sign. Further, the amplitude of the *i*th harmonic was proportional to 1/*i*. Using the electromagnetic search coil technique to record the positions of both eyes indicated that the earliest vergence eye movements elicited by these disparity stimuli had ultra-short latencies (minimum, <65 ms) and were always in the direction of the most prominent harmonic, the 3rd, but their magnitudes fell short of those elicited when the same disparities were applied to pure sinusoids whose spatial frequency and contrast matched those of the 3rd harmonic. This shortfall was evident in both the horizontal vergence responses recorded with vertical grating stimuli and the vertical vergence responses recorded with horizontal grating stimuli. When the next most prominent harmonic, the 5th, was removed from the *mf* stimulus (creating the "*mf-5*" stimulus) the vertical vergence responses showed almost no shortfall—indicating that it had been almost entirely due to that 5th harmonic—but the horizontal vergence responses still showed a small shortfall, at least with higher contrast stimuli. This small shortfall might represent a very minor contribution from higher harmonics and/or distortion products and/or a feature-based mechanism. We conclude that the earliest disparity vergence responses—especially vertical—were strongly dependent on the major Fourier components of the binocular images, consistent with early spatial filtering of the monocular visual inputs prior to their binocular combination as in the disparity-energy model of complex cells in striate cortex [Ohzawa, I., DeAngelis, G.C., & Freeman, R.D. (1990). Stereoscopic depth discrimination in the visual cortex: neurons ideally suited as disparity detectors.*Science, 249*, 1037–1041].

Keywords

Disparity energy; missing fundamental; spatiotemporal filtering

1. Introduction

When large random-dot patterns are viewed dichoptically and then suddenly subjected to small binocular misalignments (disparities), corrective vergence eye movements are elicited at ultra-short latencies, <80 ms in humans and <60 ms in monkeys (Busettini, Fitzgibbon & Miles, 2001; Busettini, Miles & Krauzlis, 1996; Masson, Busettini & Miles, 1997; Masson, Yang & Miles, 2002; Takemura, Inoue & Kawano, 2002a; Takemura, Inoue, Kawano, Quaia & Miles,

Address correspondence to: B.M. Sheliga, Laboratory of Sensorimotor Research, National Institutes of Health, Building 49 Room 2A50, 49 Convent Drive, Bethesda MD 20892-4435 USA, Tel: 301-402-4962, Fax: 301-402-0511, email: bms@lsr.nei.nih.gov.

2001; Takemura, Kawano, Quaia & Miles, 2002b; Yang, FitzGibbon & Miles, 2003). Thus, in the horizontal domain, crossed disparities elicit convergence and uncrossed disparities elicit divergence, while in the vertical domain, left-hyper disparities elicit left sursumvergence and right-hyper disparities elicit right sursumvergence, exactly as expected of a negative-feedback mechanism using binocular disparity to eliminate vergence errors. However, with broadband stimuli like dense random-dot patterns, this mechanism has a very limited range of disparities over which it behaves like a servo, so that increases in disparity result in roughly linear increases in the vergence response only with disparities up to ~2°. Indeed, disparities >4° are without effect at short latency. Thus, only small misalignments of the two eyes can be corrected by this ultra-rapid vergence mechanism, commensurate with mediation by disparity detectors that perform only local stereo matches. Vergence responses can also be elicited at ultra-short latencies by binocular disparities applied to dense anticorrelated random-dot patterns—in which the dots seen by the two eyes have opposite contrast (Masson et al., 1997; Takemura et al., 2001)—even though these patterns are perceived as rivalrous and do not support depth perception (Cogan, Kontsevich, Lomakin, Halpern & Blake, 1995; Cogan, Lomakin & Rossi, 1993; Cumming, Shapiro & Parker, 1998; Masson et al., 1997). The initial vergence responses to these anticorrelated stimuli—like the responses of many disparity-selective neurons in striate cortex (Cumming & Parker, 1997; Ohzawa et al., 1990)—are in the reverse direction of those to normal correlated stimuli (Masson et al., 1997; Takemura et al., 2001), consistent with the idea that these eye movements derive their visual input from an early stage of cortical processing prior to the level at which depth percepts are elaborated (Masson et al., 1997). That this disparity vergence mechanism functions as a low-level automatic servo also means that it is not involved in the voluntary transfer of fixation to new depth planes, a high-level process that must involve time-consuming target selections and may require the decoding of large disparity errors (>10°) with all the attendant correspondence problems.

These characteristics of the short-latency disparity-vergence responses are consistent with the behavior of disparity-selective neurons in the primate striate cortex (Cumming & DeAngelis, 2001; Cumming & Parker, 1997; Ohzawa et al., 1990; Prince, Cumming & Parker, 2002; Prince, Pointon, Cumming & Parker, 2002), many of whose properties are well captured by the so-called disparity-energy model (Fleet, Wagner & Heeger, 1996; Ohzawa et al., 1990; Parker & Cumming, 2001; Qian, 1994; Read & Cumming, 2003; Read, Parker & Cumming, 2002). However, the medial superior temporal area of the cortex (MST) appears to play a critical rôle in the generation of the earliest disparity vergence responses, at least in monkeys: Bilateral lesions of the MST in macaques result in major impairments of these eye movements (Takemura et al., 2002a), and single unit studies indicate that the summed activity of the disparity-selective neurons in MST encodes the magnitude, direction and time course of these eye movements (Takemura et al., 2001; Takemura et al., 2002b).

The stereo matching in striate cortex relies on the local interocular correlations between the filtered signals from the two eyes and, by analogy with low-level motion detectors, the underlying disparity detectors can be thought of as 1^{st}-order, Fourier or energy-based. However, there is also evidence for stereo matching based on 2^{nd}-order, non-Fourier or feature-based mechanisms.[1] For example, Hess and Wilcox (1994) found that stereoacuity for Gabor patches depended on the spatial frequency of the carrier when the latter had fewer than 4 cycles (1^{st}-order processing) and on the scale of the Gaussian envelope when the carrier had more cycles (2^{nd}-order processing). Second-order mechanisms have also been invoked to explain our ability to perceive depth in binocular stimuli with matching monocular patches even when the features within the patches are binocularly uncorrelated and defined by texture (Frisby & Mayhew, 1978), motion (Halpern, 1991), 1-D noise (Wilcox & Hess, 1996), opposite-polarity

[1]For convenience, we clump together all mechanisms that are not 1^{st}-order and refer to them as "2^{nd}-order". It is possible that the latter are in fact separable into 2^{nd}- and 3^{rd}-order mechanisms as some have suggested for visual motion (Lu & Sperling, 1996)

luminance (Pope, Edwards & Schor, 1999b), or orthogonal orientations (Edwards, Pope & Schor, 1999;Schor, Edwards & Sato, 2001). In addition, depth can be perceived in large-field stimuli in which the binocular disparity is defined solely by contrast envelopes, which are pure 2^{nd}-order stimuli (Edwards, Pope & Schor, 2000;Langley, Fleet & Hibbard, 1998;Langley, Fleet & Hibbard, 1999). Nonlinearities can render such 2^{nd}-order stimuli visible to 1^{st}-order sensing mechanisms by introducing distortion products—indeed, this is a critical factor in some models of 2^{nd}-order stereopsis (see Langley et al., 1999, for discussion)—and it is well known that there is a compressive nonlinearity early in the visual pathway (e.g., He & Macleod, 1998;MacLeod & He, 1993;MacLeod, Williams & Makous, 1992). One critical issue, therefore, is whether these early nonlinearities suffice to explain our ability to sense 2^{nd}-order disparities or whether it is necessary to invoke the existence of additional nonlinearities. Three studies point to the importance of later (cortical) nonlinearities, consistent with the idea that there are special mechanism(s) subserving 2^{nd}-order stereopsis. Firstly, Wilcox and Hess (1996) showed that stereoacuity based on the disparity of Gaussian envelopes was severely impaired if the carriers were horizontal at one eye and vertical at the other, indicating that the extraction of the envelopes in their experiments must occur in the cortex where selectivity for orientation originates. Secondly, Langley et al. (1999) showed that the effect of prior adaptation to a 1-D grating on the perceived depth of the envelope was also selective for orientation (and spatial frequency). Thirdly, Langley at al. (1999) found that the energy of the envelope frequency needed to null a depth asymmetry in the perceived transparency with 2^{nd}-order stimuli—previously described by Langley et al. (1998)—was much greater than predicted by the pre-cortical nonlinearity.

It has long been known that human subjects can initiate vergence eye movements to binocular images whose detailed form is quite different at the two eyes (Jones & Kerr, 1972; Mitchell, 1970; Westheimer & Mitchell, 1969). However, the vergence responses in these early studies might have been simply the result of low-pass 1^{st}-order processing rather than true 2^{nd}-order processing. In fact, such low-pass characteristics might not be surprising because, under normal circumstances, large absolute disparities are generally associated with substantial blurring of the retinal images, which effectively limits their high-spatial-frequency content. More recently, Schor and colleagues used Gabor patches in the competition paradigm of Jones and Kerr (1972) and reported occasional vergence responses to patches that had orthogonal carriers or opposite luminance polarity, especially with larger disparities, i.e., the disparity of the Gaussian envelope alone could suffice to initiate vergence (Pope, Edwards & Schor, 1999a; Sato, Edwards & Schor, 2001). Most recently, Stevenson (2002) has reported that horizontal—but not vertical—vergence eye movements can be elicited by binocular disparities defined solely by contrast-modulated dynamic noise, a pure 2^{nd}-order disparity stimulus. The suggestion here is that the disparity detectors mediating vertical vergence are sensitive only to 1^{st}-order disparity stimuli and the early (pre-cortical) nonlinearities do not suffice to render these contrast modulations visible to the 1^{st}-order sensing mechanism. On the other hand, horizontal vergence eye movements can result from 2^{nd}-order disparity stimuli—probably utilizing specialized cortical nonlinearities to sense the disparity—but the latency of these responses is not known.

In the present study we sought to examine the stereo matching underlying the initial vergence responses to binocular stimuli whose 2^{nd}-order features and principal 1^{st}-order (Fourier) component had disparities of opposite sign. We will describe the initial disparity-vergence responses elicited by disparities applied to the so-called *missing fundamental* (*mf*) stimulus, which consists of a square-wave that lacks the fundamental and was first used as a visual stimulus by Campbell, Howell and Robson (1971) in psychophysical studies concerned with the harmonic content of the images. In the frequency domain, a pure square-wave is composed entirely of the odd harmonics—the 1^{st}, 3^{rd}, 5^{th}, 7^{th} etc—and the amplitude of the i^{th} harmonic is proportional to $1/i$. When a square wave is displaced ¼-wavelength, all of its harmonics are displaced by ¼ of their wavelengths, the $4n+1$ harmonics in the *for*ward direction and the $4n$

−1 harmonics in the *back*ward direction. The *mf* stimulus has the important property that when displaced ¼-wavelength, its principal Fourier component (the 3rd harmonic)—being a 4*n*−1 harmonic—is displaced by ¼ of its wavelength in the *back*ward direction. In 1982, Adelson reported that, when shifted in ¼-wavelength steps, the *mf* stimulus was often perceived to move backwards (Adelson, 1982), and this subsequently led to its use as a means of dissociating the motion of the overall pattern and the motion of its harmonics (e.g., Adelson & Bergen, 1985; Baro & Levinson, 1988; Brown & He, 2000; Georgeson & Harris, 1990; Georgeson & Shackleton, 1989). Most recently, Adelson's stimulus has been used to demonstrate the importance of the Fourier components of the motion stimulus for the initiation of the ocular following response (Miura, Matsuura, Taki, Tabata, Inaba, Kawano & Miles, 2006; Sheliga, Chen, FitzGibbon & Miles, 2005a; Sheliga, Chen, Fitzgibbon & Miles, 2006a; Sheliga, Kodaka, FitzGibbon & Miles, 2006b). A few studies have investigated the binocular fusion of *mf* gratings to investigate the importance of harmonics in stereopsis (e.g., Levinson & Blake, 1979; Mayhew & Frisby, 1981), and in the present study we have adopted Adelson's approach by using *mf* patterns that were identical at the two eyes except for a difference in phase (i.e., a binocular disparity) of ¼-wavelength. Figure 1 shows a pair of *mf* gratings with a *crossed* disparity equal to ¼ of the wavelength of the repeating pattern, so that the pattern seen by the right eye is ¼-wavelength to the left of the otherwise identical pattern seen by the left eye. The patterns seen by each eye are indicated in Fig. 1A and their luminance profiles are indicated by grey lines in Figs. 1B and C. Also shown superimposed are the luminance profiles for the 3rd harmonics (black lines in Fig. 1B), which clearly have an *uncrossed* disparity equal to ¼ of their wavelength, and the 5th harmonics (black lines in Fig. 1C), which have a *crossed* disparity equal to ¼ of their wavelength. The magnitude of the disparity of the i^{th} harmonic is proportional to 1/*i*, so that the disparity of the 3rd harmonic is 1/3rd that of the fundamental pattern, the disparity of the 5th harmonic is 1/5th etc. Of course, regular repeating patterns are fundamentally ambiguous insofar as a ¼-wavelength phase difference is exactly equivalent to a ¾-wavelength phase difference in the opposite direction. In this paper, the sign of the disparity stimulus—crossed or uncrossed, left-hyper or right-hyper—will always refer to the ¼-wavelength phase difference, which we will show invariably dictates the direction of the earliest vergence responses with pure sine-wave stimuli, consistent with the idea that the brain gives the greatest weight to the "nearest-neighbor matches". [2]

We here report the horizontal vergence responses when horizontal disparities are applied to vertical grating patterns and the vertical vergence responses when vertical disparities are applied to horizontal grating patterns.[3] The available evidence suggests that the vertical vergence response is a rapid, purely involuntary reflex response to vertical disparity and functions solely to maintain the vertical alignment of the two eyes by eliminating vertical disparity errors, whereas the horizontal vergence response has both a rapid involuntary reflex component for eliminating small horizontal vergence errors and a slower, voluntary component that functions to transfer binocular fixation between objects in different depth planes (Busettini et al., 2001;Erkelens & Collewijn, 1985a;Erkelens & Collewijn, 1985b;Erkelens & Collewijn, 1991;Stevenson, 2002;Stevenson, Lott & Yang, 1997). Horizontal vergence also differs from vertical vergence in being sensitive to a variety of non-disparity (monocular) depth cues—such as accommodation (see Judge, 1996, for review), radial optic flow (Busettini, Masson & Miles, 1997;Yang, Fitzgibbon & Miles, 1999), and complex attributes like perspective, overlay, size, and relative motion (e.g., Enright, 1987a;Enright, 1987b;Ringach, Hawken & Shapley, 1996), as well as perceived depth *per se* (Sheliga & Miles, 2003)—and in being subject to attentional modulation (Stevenson et al., 1997). Furthermore, as mentioned earlier, the

[2]In contrast, the perceived depth associated with briefly presented disparities is sometimes determined by the next-to-nearest-neighbor matches (Edwards & Schor, 1999).

[3]We shall ignore any orthogonal vergence responses (i.e., vertical vergence responses to horizontal disparities and vice versa), which are known to occur under some conditions (Busettini et al., 2001).

horizontal disparity-vergence mechanism responds to contrast-defined (i.e., pure 2nd-order) disparities whereas the vertical disparity-vergence mechanism does not (Stevenson, 2002). This last study provided only closed-loop vergence gain measures so it is not clear if such 2nd-order stimuli initiate horizontal disparity-vergence responses at short latency.

We report that the very earliest disparity-vergence responses—horizontal and vertical—elicited by ¼-wavelength stimuli applied to *mf* gratings were invariably in the backward direction, i.e., in the direction of the 3rd harmonic, consistent with early spatio-temporal filtering and mediation by 1st-order disparity-energy detectors. Two separate experiments are described, dealing with the dependence of these responses on spatial frequency and contrast, respectively. Some preliminary horizontal vergence data were previously published in a conference report (Sheliga, Chen, Fitzgibbon & Miles, 2005b).

2. Experiment 1: Dependence of initial vergence responses on spatial frequency and the harmonic content of broadband stimuli

This first experiment was concerned with the general form of the initial vergence responses elicited by ¼-wavelength disparities applied to various grating patterns and with their quantitative dependence on spatial frequency. Of course, with such regular repeating patterns a ¼-wavelength phase difference is exactly equivalent to a ¾-wavelength phase difference of the opposite sign. Our present experiments are based on the assumption that the initial vergence eye movements are produced by a negative-feedback mechanism that works to eliminate vergence errors by sensing the fixation disparity using detectors that give greatest weight to the nearest-neighbor matches, i.e., the direction of the initial vergence response with a seemingly ambiguous stimulus such as a pure sinusoidal grating is always determined by the ¼-wavelength phase difference. However, a recent study reported that the perceived depth associated with briefly presented disparities applied to 1D sinusoidal gratings—exactly as in the present study—was sometimes determined by the next-to-nearest-neighbor matches (Edwards & Schor, 1999). We will therefore first show that the initial vergence responses associated with pure sine-wave stimuli always operated to reduce the ¼-wavelength phase differences, before going on to report our findings with more complex broadband patterns such as the *mf* stimulus. We also used an *mf* stimulus that lacked the 5th harmonic (*mf-5* stimulus) to help define the rôle of that harmonic.

2.1. Methods

Some of the techniques, such as those used for recording eye movements and for data analysis, were very similar to those used previously in our laboratory (Sheliga et al., 2005a; Yang et al., 2003) and, therefore, will be described only in brief here. Experimental protocols were approved by the Institutional Review Committee concerned with the use of human subjects.

2.1.1. Subjects—Three subjects participated; two were authors (BMS, FAM) and the third was a paid volunteer who was unaware of the purpose of the experiments (NPB). Inter-pupillary distances were 68.5, 68, and 67 mm, respectively. All subjects had normal or corrected-to-normal vision.

2.1.2. Visual display and the grating stimuli—The subjects sat in a dark room with their heads positioned by means of adjustable rests for the forehead and chin, and held in place with a head band. Dichoptic stimuli were presented using a Wheatstone mirror stereoscope. Each eye viewed a computer monitor through a 45° mirror, creating a single binocular surface straight ahead at 47.1 cm from the eye's corneal vertex, which was also the optical distance to the images on the monitor screen. Stimuli were displayed on Sony GDM-F520 21" CRT monitors driven by a PC Radeon 9800 Pro video card. The monitor screen was 400 mm wide

× 300 mm high (subtense, 46 ° × 35°), with 1600 by 1200 pixels, and a vertical refresh rate of 70 Hz. Using a video signal splitter (Black Box Corp., AC085A-R2), the "red" video signal was connected to all three RGB inputs to the monitor viewed by the left eye, and the "green" signal was connected to all three RGB inputs to the monitor viewed by the right eye. This arrangement allowed the presentation of independent black and white images simultaneously to each eye. Images with a greyscale resolution up to eleven bits were produced using a Bits+ + Digital Video Processor (Cambridge Research Systems Ltd.) inserted between the PC video card and the splitter. Two luminance look-up tables (one for each monitor) with 64 equally-spaced luminance levels ranging from 0 cd/m^2 to 77.4 cd/m^2 were created by direct luminance measurements (IL1700 photometer; International Light Inc., Newburyport, MA) under custom software control. Each table was then expanded to 2048 equally-spaced levels by interpolation and thereafter luminance was checked regularly for linearity at 2- or 3-week intervals (typically, r^2=0.99997).

In one series of recordings, the visual images consisted of one-dimensional vertical grating patterns that could have one of three horizontal luminance profiles in any given trial: 1) a pure sine wave, 2) a square wave without a 1st harmonic (the *mf* stimulus), 3) a square wave without either a 1st or a 5th harmonic (the *mf-5* stimulus). Images were identical for the two eyes except for a horizontal phase difference that was ¼ of the wavelength of the pattern (with either crossed or uncrossed disparity). However, the absolute position of the pair of gratings was randomized from trial to trial at intervals of 1/8 of the wavelength of the pattern. Each image extended out to the boundaries of the screen. The dependent variable in this first experiment was the spatial frequency of the gratings, randomly sampled each trial from a lookup table. For the pure sine-wave stimuli, the entries in the table were: 0.0647, 0.129, 0.172, 0.259, 0.517, 1.034, 2.069, and 4.138 cycles/°. (Subject FAM wore spectacles with a magnification factor of 1.18 for horizontal and 1.17 for vertical and the plotted values for spatial frequency reflect this.) For the *mf* and *mf-5* stimuli, the entries in the table were: 0.0431, 0.0575, 0.0862, 0.172, 0.345, 0.690, and 1.379 cycles/°, so that the spatial frequencies of their 3rd harmonics matched those of the pure sine-wave stimuli. (Subjects BMS and FAM ran an additional three spatial frequencies in the horizontal disparity experiments: 0.0431 and 0.0862 cycles/° pure sine-wave stimuli and 0.0287 cycles/° *mf* and *mf-5* stimuli.) The contrasts of the *mf* and *mf-5* stimuli were adjusted so that the Michelson contrasts of their 3*f* components matched those of the pure sinusoids, which were always 32%. A second series of recordings used visual stimuli that were the same except for their orthogonal orientation, i.e. vertical disparities were applied to horizontal grating patterns.

The visual displays had a resolution of 33.1 pixels/°, so that any components of the stimuli with spatial frequencies greater than 16.55 cycles/° (the Nyquist Frequency) would be aliased to lower frequencies. To avoid spatial aliasing, the *mf* and *mf-5* stimuli were synthesized by summing the requisite odd harmonics and including only those with spatial frequencies below the Nyquist Frequency: see Sheliga et al. (2005a) for detailed discussion. Note that all spatial frequencies given in this paper refer to the value at the point on the (tangent) screen directly ahead of each eye.

2.1.3. Eye-movement recording—The horizontal and vertical positions of both eyes were recorded with an electromagnetic induction technique (Robinson, 1963) using scleral search coils embedded in silastin rings (Collewijn, Van Der Mark & Jansen, 1975), and each was sampled at 1-ms intervals as described by Yang, FitzGibbon and Miles (2003).

2.1.4. Procedures—All aspects of the experimental paradigms were controlled by two PCs, which communicated via Ethernet using the TCP/IP protocol. One of the PCs was running a Real-time EXperimentation software package (REX) developed by Hays, Richmond and Optican (1982), and provided the overall control of the experimental protocol as well as

acquiring, displaying, and storing the eye-movement data. The other PC was running Matlab subroutines, utilizing the Psychophysics Toolbox extensions (Brainard, 1997; Pelli, 1997), and generated the visual stimuli upon receiving a start signal from the REX machine.

At the beginning of each recording session, the horizontal and vertical signals from each eye coil were calibrated separately by having the subject fixate monocular targets presented at known eccentricities along the horizontal and vertical meridians. After completing the calibrations, the experiment proper began. The subject was instructed to fixate a binocular central black target cross (1° high × 5° wide × 0.21° thick) that appeared at the beginning of each trial at the center of an otherwise uniform grey screen (luminance, 38.7 cd/m^2). After the subject's two eyes had each been positioned within 2° of the center of its fixation cross and no saccades had been detected (using an eye velocity threshold of 18°/s) for a randomized period of 800 to 1100 ms both crosses disappeared and were immediately replaced by grating patterns (randomly selected from a lookup table); these patterns were identical for the two eyes except for a phase difference of ¼-wavelength, and filled the screens for 200 ms. At this point the screens were blanked (luminance, 38.7 cd/m^2), marking the end of the trial. After an inter-trial interval of 500 ms, the binocular fixation cross reappeared, commencing a new trial. The subjects were asked to refrain from blinking or making any saccades except during the inter-trial intervals but were given no instructions relating to the disparity stimuli. If no saccades were detected during the period of the trial, then the data were stored on a hard disk; otherwise, the trial was aborted and subsequently repeated. Each block of trials had 44–52 randomly interleaved stimulus combinations: 3 grating patterns, each with 7–10 spatial frequencies (indicated above), and the disparity could have 2 signs. Data were collected over several sessions until each condition had been repeated an adequate number of times to permit good resolution of the responses (through averaging). The actual numbers of trials will be given in the Results. Two separate experiments were carried out: in one, the gratings were vertical and the disparities could be crossed or uncrossed, and in the other the gratings were horizontal and the disparities could be left-hyper or right-hyper.

2.1.5. Data analysis—The horizontal and vertical eye-position measures obtained during the calibration procedure were each fitted with second-order polynomials which were then used to linearize the corresponding eye-position data recorded during the experiment proper. The linearized eye-position measures were smoothed with a 6-pole Butterworth filter (3 dB at 45 Hz) and then mean temporal profiles were computed for each stimulus condition. Trials with saccadic intrusions (that had failed to reach the eye-velocity threshold of 18°/s during the experiment) were deleted. We used the convention that rightward and upward deflections of the stimuli or eyes were positive. The horizontal (vertical) vergence angle was computed by subtracting the horizontal (vertical) position of the right eye from the horizontal (vertical) position of the left eye. This meant that *con*vergence and *left*-sursumvergence had positive signs. To improve the signal-to-noise, the mean vergence response profile to each uncrossed (right-hyper) disparity stimulus was subtracted from the mean vergence response profile to the corresponding crossed (left-hyper) disparity stimulus. As convergence and left sursumvergence were positive in our sign convention, these pooled horizontal (vertical) difference measures were positive when in the forward/compensatory/corrective direction. The initial vergence responses in each stimulus condition were quantified by measuring the *changes in these pooled vergence position measures* over the 50-ms time periods commencing 60 ms after the onset of the disparity stimuli. The minimum latency of vergence onset was slightly greater than 60 ms from the first appearance of the disparity stimuli so that these vergence-response measures were restricted to the initial open-loop period.

2.2. Results

2.2.1. Initial vergence responses to pure sine-wave stimuli—The direction of the initial vergence responses with pure sine-wave stimuli was always as expected of a negative-feedback mechanism operating to eliminate the ¼-wavelength phase difference. This is apparent from the sample mean vergence velocity profiles in Fig. 2 obtained from subject NPB: when the sign of the disparity stimuli was defined by the ¼-wavelength phase differences, crossed disparities resulted in convergent responses (Fig. 2A), uncrossed disparities resulted in divergent responses (Fig. 2C), left-hyper disparities resulted in left sursumvergence (Fig. 2B) and right-hyper disparities resulted in right sursumvergence (Fig. 2D), all with minimum onset latencies <65 ms. It was also significant that the distributions of the individual vergence responses to a given disparity stimulus were always well fitted by Gaussian functions, consistent with unimodal response distributions: for all subjects, the mean r^2 values for the best-fit Gaussian functions for the vergence responses to all sine-wave stimuli exceeded 0.90. In addition, when a given stimulus was of sufficient efficacy, responses to that stimulus all had the same direction: see, for example, the histograms in Fig. 2E, which show the distributions of the horizontal vergence responses to ¼-wavelength crossed and uncrossed disparities applied to sine-wave gratings of spatial frequency 0.26 cycles/°. The corresponding vertical data in Fig. 2F were similarly polarized (though, in this case, the spatial frequency of the stimuli was 0.52 cycles/°, and 1 of 135 responses to the right-hyper stimulus was in the "wrong" direction—left sursumvergence).

The vergence responses to disparities of opposite polarity—crossed versus uncrossed, or left-hyper versus right-hyper—generally showed only minor, idiosyncratic, differences: compare A and C (also B and D) in Fig. 2. In order to improve the signal-to-noise ratio, we pooled the mean data for the two stimulus polarities by subtracting the mean response to a given uncrossed (right-hyper) disparity from the mean response to the corresponding crossed (left-hyper) disparity. Samples of the resultant mean pooled vergence velocity profiles (obtained from subject NPB) in response to ¼-wavelength disparities applied to pure sine-wave stimuli of various spatial frequencies are shown in Figs. 3A (horizontal responses to horizontal disparities) and 3D (vertical responses to vertical disparities). Note that all deflections in Fig. 3A, D are *up*ward indicating that responses had a *positive* sign signifying that the mean vergence responses always operated to reduce the imposed ¼-wavelength disparity, i.e., to reduce the disparity of the nearest-neighbor matches. We shall refer to such responses as *forward, compensatory or corrective*, consistent with the operation of a negative-feedback control system using local disparity signals to eliminate local vergence errors.

The open circles plotted in Fig. 4 show the quantitative dependence of pooled vergence responses such as those in Fig. 3A, D on log spatial frequency (based on the changes in the mean pooled vergence position measures over the 50-ms time period starting 60 ms after stimulus onset) for all three subjects, with the horizontal data above (A–C) and the vertical data below (D–F). It is clear that with the pure sine-wave stimuli these vergence response measures were always positive and displayed a band-pass dependence on log spatial frequency that was well captured by Gaussian functions (continuous smooth curves in Fig. 4), for which the r^2 values were always >0.98. The three parameters of the best-fit Gaussian functions—peak amplitude (A_{peak}), spatial frequency of the peak (f_o) and standard deviation (σ)—are listed in Table 1, together with the low-frequency cutoff (f_{lo}) and the high-frequency cutoff (f_{hi}), which are the spatial frequencies at which the tuning curve was half its maximum: see Read and Cumming (2003) for their derivation. It is apparent that the vertical vergence data consistently peaked at a higher spatial frequency and had a slightly narrower bandwidth than the horizontal vergence data: mean difference in f_o, 0.14 cycles/°, and mean difference in σ, 0.04 log cycles/°.

2.2.2. Initial vergence responses to broadband (mf and mf-5) stimuli—The earliest vergence responses elicited by ¼-wavelength disparities applied to the *mf* and *mf-5* broadband stimuli also had minimum onset latencies <65 ms but were invariably in the *back*ward direction, i.e., in the direction of the principal Fourier component, the 3rd harmonic. This is evident from the *down*ward deflections of the mean pooled vergence velocity profiles from subject NPB shown in Fig. 3 (B, E: *mf* data; C, F: *mf-5* data), as well as from the *negative* values of the mean pooled vergence position measures for all three subjects plotted in Fig. 4 (*mf* data: open squares and continuous lines; *mf-5* data: closed diamonds and dashed lines). Like the data obtained with sine-wave stimuli, those obtained with the broadband stimuli showed a band-pass dependence on spatial frequency that was again well captured by Gaussian functions when plotted on a log abscissa (in all cases, $r^2>0.95$), though this is somewhat less apparent for the horizontal vergence data for subjects NPB and BMS because their broadband data lack an adequate number of samples for frequencies below the peak. In fact, it is evident from Fig. 4 and from the values of f_o listed in Table 1 that the data obtained with the broadband stimuli generally peaked at spatial frequencies that were only about 1/3rd of those for the data obtained with the pure sine-wave stimuli.

Such a difference in the spatial-frequency tuning of the data obtained with broadband and pure sine-wave stimuli would be expected if the former resulted mainly from the disparity of the principal Fourier component, the 3rd harmonic, rather than the disparity of the overall pattern. Further, if the responses to the broadband gratings were *solely* determined by their 3rd harmonic then, when replotted as a function of the spatial frequency of that harmonic, the data obtained with broadband stimuli should show the same dependence on spatial frequency as those obtained with the pure sine-wave stimuli.[4] When so replotted, the spatial-frequency dependencies of the data obtained with the broadband stimuli were sometimes strikingly similar to those obtained with the pure sine-wave stimuli, especially for the vertical vergence data obtained with the *mf-5* stimuli. To illustrate this and facilitate easy comparison, in Fig. 4 we have replotted the best-fit Gaussian functions for the data obtained with the broadband stimuli as a function of the spatial frequency of their 3rd harmonic *with a sign inversion*, with the *mf* data shown in continuous grey lines and the *mf-5* data in dashed grey lines. The parameters of the best-fit Gaussian functions for the replotted vergence data are listed in parentheses in Table 1, and indicate that the vertical vergence data obtained from all 3 subjects with the *mf-5* stimuli almost matched those for the data obtained with the corresponding sine-wave stimuli. The equivalent horizontal vergence data obtained with the *mf-5* stimuli showed the same trends but were generally of lower amplitude than the data obtained with corresponding pure sine-wave stimuli (mean difference in A_{peak}, 15%) and, in two subjects (NPB, BMS), peaked at a slightly lower spatial frequency (Fig. 4A–C and Table 1). The replotted data obtained with the *mf* stimuli generally peaked at a similar spatial frequency—but reached a lower amplitude than —the corresponding *mf-5* data, and these amplitude differences were a little more pronounced for the horizontal data (mean difference in A_{peak} for the *mf* and *mf-5* data, 22%) than for the vertical data (mean difference in A_{peak} for the *mf* and *mf-5* data, 12%).

2.3. Discussion of Experiment 1

The disparity vergence responses under study here are assumed to result from the operation of a negative-feedback servo mechanism that uses fixation disparity as an index of vergence errors to maintain binocular alignment of the eyes. When confronted with pure sine-wave disparity stimuli that were potentially ambiguous—differing in phase at the two eyes by ¼ wavelength and so also definable as a ¾-wavelength phase difference with the opposite sign—the resulting vergence eye movements always operated to reduce the binocular disparity of the lesser of the

[4]Note that the contrasts of the broadband stimuli were such that their 3rd harmonics always had the same contrast as the pure sine-wave gratings: 32%.

two phase differences (Fig. 2). This is consistent with the idea that the relevant disparity detectors give greatest weight to the nearest-neighbor matches. Whether using pure sine-wave stimuli or the *mf* and *mf-5* broadband stimuli, the earliest vergence eye movements had minimum latencies <65 ms and showed a band-pass dependence on spatial frequency that was well fit by a Gaussian function (on a log abscissa). However, when applied to *mf* and *mf-5* stimuli these ¼-wavelength disparities generated vergence eye movements that always started in the "wrong" direction, operating to increase the ¼-wavelength disparity of the whole pattern, and peaked at a much lower spatial frequency than the data obtained with pure sine-wave stimuli (Figs. 3, 4). One possible explanation for this difference in the sign and in the spatial frequency tuning is that the system was actually responding to the disparity of the principal Fourier component, the 3rd harmonic, which had the opposite sign and a spatial frequency three times that of the overall pattern. This would be the behavior expected of a low-level mechanism that senses the 1st-order disparity energy, as in the so-called disparity-energy model that has been invoked to explain the disparity-selective behavior of complex cells in striate cortex (Ohzawa et al., 1990). When replotted as a function of the spatial frequency of that 3rd harmonic (and inverted), some of the data obtained with broadband stimuli came close to matching the data obtained with pure sine-wave stimuli whose contrast and spatial frequency matched those of the 3rd harmonic, but other data fell short. This shortfall was much more evident in the horizontal vergence data than in the vertical and we will discuss them separately.

2.3.1. Vertical vergence—The replotted vertical vergence data obtained with the *mf-5* stimuli showed a dependence on spatial frequency that was very close to that obtained with the pure sine-wave stimuli, with an average shortfall in amplitude of only 7%. This finding is consistent with the idea that the vertical vergence responses to the *mf-5* disparity stimuli are due almost entirely to the 3rd harmonic and are as expected of a mechanism that responds to the 1st-order disparity energy. These *mf-5* data also indicate that almost all of the shortfall in the vertical *mf* data could be attributed to the 5th harmonic, which was the largest of the 4*n*+1 harmonics whose ¼-wavelength phase difference at the two eyes had the opposite sign to the 3rd harmonic (Fig. 1B, C). The slight shortfall in the *mf-5* data might reflect the influence of a number of factors: 1) higher harmonics, 2) distortion products that result from compressive nonlinearities in the visual pathway, and 3) a feature-based mechanism. We will consider each in turn.

The next largest harmonic after the 5th is the 7th, which like the 3rd is a 4*n*−1 harmonic and might therefore be expected to *decrease* the shortfall. However, in a recent study we used *mf-5* motion stimuli to elicit ocular following and found that additionally *removing* the 7th harmonic ("*mf-5&7* stimulus") actually *increased* the response in the direction of the 3rd harmonic very slightly (Sheliga et al., 2005a). We suggested that if ocular following were to respond to the average speed of the harmonics then the 7th harmonic might actually work to diminish the impact of the 3rd harmonic because the apparent speed of the 7th is only 43% of that of the 3rd. However, in a more recent study of ocular following we showed that there are major nonlinear interactions (mutual inhibition) between the mechanisms sensing the different harmonics that can bias responses strongly in favor of the harmonic with the highest contrast (Sheliga et al., 2006b). Using just two competing sine waves equivalent to the 3rd and 5th (or the 3rd and 7th) harmonics of the broadband stimuli we found that when the two differed in contrast by more than an octave then the one with the lower contrast completely lost its influence (winner-take-all) but when their contrasts were more similar then both continued to exert an influence (vector sum/averaging). We have preliminary evidence (unpublished observations) that similar—though perhaps less powerful—nonlinear interactions occur between the neural mechanisms sensing the disparity of the different harmonics in our present experiments. The implication is that the 3rd harmonic of the *mf* stimuli, having the highest contrast, would actively work to reduce the impact of the higher harmonics that had appreciably lower contrasts.

Our earlier study on ocular following (Sheliga et al., 2005a) also showed that when the *mf* and *mf-5* stimuli are subject to compressive nonlinearities (such as others have proposed occur early in the visual pathway) there are distortion products that consist mostly of the even harmonics, i.e., the 2nd, 4th, 6th et seq. Given that the disparity of the *i*th even harmonic of the *mf* and *mf-5* stimuli is *i*/4 multiples of its wavelength, some distortion products will be seen by the two eyes exactly counterphase (e.g., the 2nd, 6th, 10th etc., harmonics) whereas others will be seen by the two eyes exactly in phase (e.g., the 4th, 8th, 12th etc., harmonics), i.e., zero disparity. Our earlier analysis also revealed that, in general, the amplitudes of the distortion products associated with the *mf-5* stimuli were smaller than those associated with the *mf* stimuli, e.g., the most prominent distortion products were the 2nd and 4th harmonics, and their amplitudes (expressed as a percentage of the amplitude of the 3rd harmonic) were 35% and 28%, respectively, with the *mf* stimuli, and 12% and 20%, respectively, with the *mf-5* stimuli.[5] Clearly, such distortion products might work to attenuate the vergence responses to the odd harmonics of the broadband stimuli but it is also possible that the non-linear interactions alluded to above might work to reduce their influence. In general, however, given that the vertical vergence data obtained with the *mf-5* and pure sine-wave stimuli are so similar, the net effects of higher harmonics and distortion products can only be very small. Likewise, at best, feature-based mechanisms can make only a very modest contribution to the vertical vergence responses.

2.3.2. Horizontal vergence—The replotted spatial frequency tuning curves for the horizontal vergence data obtained with the *mf-5* stimuli not only fell a little short of those obtained with pure sine-wave stimuli that matched the 3rd harmonic but, in 2/3 subjects, also peaked at a slightly lower spatial frequency (Fig. 4A–C). The clear suggestion is that, although the principal Fourier component is the major factor in the genesis of the horizontal vergence responses, one or more of the other three factors mentioned above—higher harmonics, distortion products, and feature-based mechanisms—must exert a greater influence on the horizontal vergence eye movements than on the vertical. It seems likely that the higher harmonics and distortion products are comparable for horizontal and vertical vergence, implying that the differences are in the contribution of feature-based mechanisms.[6] As pointed out in the Introduction, contrast-defined disparity stimuli, which are purely 2nd-order, can elicit horizontal—but not vertical—vergence (Stevenson, 2002). This last study considered only steady-state responses to disparities that were sinusoidally modulated over time, hence it is not known if the responses to 2nd-order disparity can be elicited at short latency, nor if they utilize a mechanism that can sense the 2nd-order features in our broadband stimuli.

2.3.3. Dependence on spatial frequency and/or binocular disparity?—Although we have described our vergence responses in terms of their dependence on spatial frequency, our stereo pairs always differed in phase by a ¼-wavelength and hence the magnitude of the disparity—an important determinant of the vergence response—always co-varied (inversely) with the spatial frequency. Thus, the data in Fig. 4 are not like the usual "tuning curves" for spatial frequency or disparity. In Fig. 4 the abscissas indicate both the spatial frequency (in cycles/°) and the disparity (in degrees), the latter being ¼ of the reciprocal of the former. Interestingly, the disparities at which the Gaussian functions in Fig. 4 peaked with the pure sine-wave stimuli (ranges: 1.00°–1.24° for the horizontal data and 0.66°–0.77° for the vertical data) compare closely with those reported for broadband (random-dot) stimuli (Busettini et al., 2001).

[5]In the analysis of Sheliga et al. (2005a), the distortion products associated with the pure *3f* stimulus were simple multiples (*6f*, *9f* etc.) with progressively decreasing amplitude, so that the most powerful one (*6f*) was the only one with significant contrast (~3.3%).

[6]Although there might be differences in the strengths of the nonlinear interactions in the horizontal and vertical sensing mechanisms that might also be expected to influence the relative contributions of the various harmonics.

3. Experiment 2: Dependence of initial vergence responses on contrast

Experiment 1 indicated that the initial vergence responses elicited by ¼-wavelength disparity steps applied to the *mf* and *mf-5* stimuli were strongly dependent on the principal Fourier components and showed a band-pass dependence on spatial frequency. In the present experiment we examined these responses further by investigating their dependence on contrast and were especially interested in comparing the vergence responses elicited by the *mf* and *mf-5* stimuli with those elicited when identical steps were applied to pure sine-wave gratings with spatial frequencies that matched those of the 1*f* and 3*f* components of the broadband stimuli.

3.1. Methods

The subjects, as well as most of the methods and procedures, were identical to those used in Experiment 1, and only those that were different will be described here.

3.1.1. Visual display—Four types of horizontal and vertical gratings were used: two broadband stimuli—*mf* and *mf-5*—and two pure sine-wave gratings—the "*1f* stimulus" (whose spatial frequency equaled that of the fundamental frequency of the *mf* and *mf-5* stimuli) and the "*3f* stimulus" (whose spatial frequency equaled that of the 3rd harmonic of the *mf* and *mf-5* stimuli). Spatial frequencies were selected so that the *1f* and *3f* stimuli were of comparable efficacy, i.e., they were symmetrically located on either side of the peaks in the spatial frequency tuning curves obtained with pure sine-wave gratings (Fig. 4). Accordingly, the fundamental spatial frequencies of the vertical gratings were 0.125, 0.146, and 0.118 cycles/° for subjects BMS, FAM, and NPB, respectively, and of the horizontal gratings were 0.218, 0.186, and 0.218 cycles/° for the same three subjects, respectively. The disparities were always ¼ of the fundamental wavelength of the *mf*, *mf-5* and *1f* stimuli (and, hence, ¾ of the wavelength of the *3f* stimuli and of the 3rd harmonics of the broadband stimuli). The dependent variable was the Michelson contrast, randomly sampled each trial from a lookup table. The contrast values in the lookup table for the *1f* and *3f* stimuli were 0.5%, 1%, 2%, 4%, 8%, 16%, 32%, and 64%. The contrasts of the *mf* and *mf-5* stimuli were selected so that the contrasts of their 3*f* components matched the contrasts of the *3f* stimuli (up to a maximum of 32%). To avoid spatial aliasing, these stimuli were synthesized up to the Nyquist Frequency (≤16.55 cycles/°), so that the highest harmonics (75th–139th) had a contrast of only 0.69–1.28%, which we estimate is close to the threshold for disparity vergence (see Fig. 6).

3.1.2. Procedures—These were as in Experiment 1 except that each block of trials had 60 randomly interleaved stimulus combinations: 4 grating patterns, each with 7 or 8 contrasts (indicated above) and the disparity could have 2 signs. Two separate experiments were carried out: in one, the gratings were vertical and the disparities could be crossed or uncrossed, and in the other the gratings were horizontal and the disparities could be left-hyper or right-hyper.

3.2. Results

The initial vergence responses elicited by ¼-wavelength disparities applied to *mf* and *mf-5* stimuli were again always in the direction of the 3rd harmonic, this time over the full range of contrasts to which the subjects were responsive. Sample mean pooled vergence velocity profiles from one subject are shown in Fig. 5—as in Fig. 3, these profiles were obtained by subtracting the mean response to a given uncrossed (right-hyper) disparity from the mean response to the corresponding crossed (left-hyper) disparity—and all the horizontal vergence data are shown above (Fig. 5A–D) while the vertical vergence data are below (Fig. 5E–H). Note that the two numbers printed to the right of the *mf* and *mf-5* traces indicate the contrasts of the associated patterns and of their 3rd harmonics (the latter in parentheses). Also shown in Fig. 5 for comparison are the vergence responses elicited when the *same disparities* were

applied to the pure sine-wave stimuli, which were all in the expected direction: forward with the *1f* stimuli (upward deflections in Fig. 5A, E) and backward with the *3f* stimuli (downward deflections in Fig. 5B, F).

The quantitative dependence on contrast, based on the mean pooled vergence position measures, was quite similar in all subjects: see the plots in Fig. 6, in which the horizontal vergence data are above (A–C) and the vertical below (D–F). With the *1f* and *3f* stimuli (closed and open circles, respectively, in Fig. 6), the responses of each of the 3 subjects showed a monotonic rise from a threshold contrast of ~1% and were each fitted with the following expression:

$$R_{\max}\frac{c^n}{c^n+c_{50}^n}; \quad (1)$$

where R_{max} is the maximum attainable response, c is the contrast, c_{50} is the semi-saturation contrast (at which the response has half its maximum value), and n is the exponent that sets the steepness of the curves. This expression is based on the Naka-Rushton equation (Naka & Rushton, 1966) and various studies have shown that it provides a good fit to the contrast dependence curves of neurons in the LGN, V1 and MT of monkeys (e.g., Albrecht, Geisler, Frazor & Crane, 2002;Albrecht & Hamilton, 1982;Heuer & Britten, 2002;Sclar, Maunsell & Lennie, 1990), as well as the initial human ocular following responses to moving sine-wave gratings (Masson & Castet, 2002;Sheliga et al., 2005a). The continuous smooth lines in Fig. 6 are the best fit curves using expression 1 and are excellent approximations to the data (mean r^2, 0.99). The parameters, c_{50} and n, for these various fits are printed beside the curves in Fig. 6. For the vertical vergence data, the best-fit curves for the *3f* and *1f* data are virtually identical: mean absolute differences in c_{50} and n for a given subject are 1.3% and 0.05, respectively. These same values are somewhat higher for the horizontal data—21% and 0.23, respectively—mainly because of subject BMS's *3f* data. The horizontal and vertical vergence data obtained with the pure sine-wave stimuli were generally very similar. This was particularly so for the *1f* data, for which the mean values for c_{50} and n for the three subjects were 13% and 1.16 for the horizontal, 13% and 1.12 for the vertical. The values for the corresponding *3f* data were 33% and 0.93 for the horizontal, 13% and 1.13 for the vertical.

The contrast response data for the *mf* stimuli (grey open squares and dotted lines in Fig. 6) and for the *mf-5* stimuli (grey filled diamonds and dashed lines in Fig. 6) lie to the right of the data obtained with the *3f* stimuli, which again is perhaps not surprising if the responses are driven mainly by the disparity of the 3rd harmonic rather than the disparity of the overall pattern. If the responses to the *mf* and *mf-5* gratings were solely determined by their 3rd harmonic then, when replotted as a function of the contrast of this harmonic, the *mf* and *mf-5* data should show the same dependence on contrast as the *3f* sine-wave data. When so replotted the *mf* and *mf-5* data do closely follow the data obtained with the *3f* stimuli at low contrasts—especially the vertical vergence data—but gradually fall increasingly short as contrast exceeds 4–8% (*mf* stimulus) or 8–16% (*mf-5* stimulus): see the black open squares and black filled diamonds in Fig. 6. At the highest contrast available for the broadband data (contrast of 3rd harmonic, 32%), the replotted *horizontal* vergence data obtained with the *mf* stimulus were on average 51% less than the corresponding data obtained with the pure *3f* stimulus, and for the *mf-5* data this shortfall averaged only 15%. These same shortfalls for the replotted *vertical* vergence data were only 20% with the *mf* stimulus and a mere 5% with the *mf-5* stimulus.

3.3. Discussion of Experiment 2

The initial vergence responses elicited by the *mf* and *mf-5* stimuli were always in the direction of the principal Fourier component, the 3rd harmonic, and when plotted in terms of the contrast of this harmonic, their amplitudes generally matched those obtained with the *3f* stimuli for

contrasts up to 4–8% but fell progressively short with higher contrasts (Fig. 6). The *mf-5* data indicate that, once again, much of the shortfall in the *mf* data was due to the 5th harmonic whose amplitude is second only to that of the 3rd harmonic. In fact, the *mf-5* data fell short of the data obtained with the pure *3f* stimulus only at higher contrasts, the shortfall at the highest contrast reaching an average of only 15% for the horizontal vergence data and a mere 5% for the vertical vergence data. This strongly suggests that the *vertical* vergence responses elicited by the broadband stimuli were almost completely determined by the principal Fourier components and any contribution from feature-based mechanisms was exceedingly small. The possibility exists of a weak feature-based contribution to the *horizontal* vergence data obtained with the broadband stimuli, perhaps consistent with other data indicating that the horizontal vergence mechanism responds to a much wider range of stimuli than the vertical mechanism, including 2nd-order disparity and a variety of non-disparity stimuli (see Introduction for references). Of course, some (perhaps even all) of the slight shortfall in the horizontal vergence data obtained with the *mf-5* stimuli at higher contrasts might be due to the higher harmonics and/or distortion products—though, as explained earlier, there are probably nonlinear interactions between the mechanisms sensing the different harmonics which reduce the efficacy of the higher ones because their contrasts are so much lower than that of the 3rd harmonic. Interestingly, Scott-Samuel and Georgeson (1999) used a nulling technique to show that the distortion products associated with 2nd-order motion stimuli (defined by a contrast-modulated carrier) increased as the square of the contrast, exactly as predicted by the compressive nonlinearity that they and we (Sheliga et al., 2005a) used to model distortion products. This might be one reason why the *mf-5* data fell increasingly short of the pure *3f* data as contrast increased, though it seems unlikely that the horizontal and vertical vergence mechanisms would differ in their sensitivity to higher harmonics and distortion products. Regardless, any contribution from feature-based mechanisms is at best very minor and, as in Experiment 1, the vergence responses were largely determined by the principal Fourier components of the disparity stimuli consistent with early spatial filtering prior to binocular matching as in the disparity energy model of V1 complex cells (Ohzawa et al., 1990).

4. Closing remarks

As pointed out in the Introduction, there is strong evidence that the medial superior temporal area of the cortex (MST) plays a critical rôle in the generation of the earliest disparity vergence responses, and this dependence on MST is also shared by two other kinds of eye movements that are elicited at ultra-short latencies by large-field visual stimuli (Takemura et al., 2002a): the ocular following response (OFR), which generates version eye movements in response to motion in the plane of fixation (Gellman, Carl & Miles, 1990; Masson, Busettini, Yang & Miles, 2001; Miles, Kawano & Optican, 1986), and the radial-flow vergence response (RFVR), which generates vergence eye movements in response to radial optic flow (Busettini et al., 1997; Yang et al., 1999). Recent studies in our laboratory indicate that these eye movements, which earlier studies showed have much in common with the disparity vergence eye movements in the present study (see Miles, 1998, for review of the earlier work), also depend heavily on the Fourier composition of the stimulus used to generate them (Kodaka, Sheliga, FitzGibbon & Miles, 2005; Sheliga et al., 2005a; 2006a; 2006b). The current study indicates two more features that all 3 eye movements have in common: band-pass spatial frequency tuning that is well represented by a Gaussian function, and contrast dependence that shows a gradual saturation well represented by the Naka-Rushton function. Even some of the quantitative details are quite similar. For example, the mean parameters of the best-fit Gaussian functions for the spatial frequency tuning curves for our horizontal vergence data obtained with pure sinusoids (f_0=0.22 cycles/°; σ=0.46 log units) compare reasonably well with those for the horizontal OFR (f_0=0.25 cycles/°; σ=0.51 log units) and the RFVR (f_0=0.29 cycles/°; σ=0.65 log units). However, this was not so of the contrast dependency. For example, the mean parameters of the best-fit Naka-Rushton functions for our horizontal vergence data obtained

with *1f* stimuli (C_{50}=14%; n=1.1) indicated a much more gradual saturation with contrast than was reported for the horizontal OFR (C_{50}=4%; n=2.1) and the RFVR (C_{50}=2%; n=1.6). The early saturation seen in the OFR and the RFVR is characteristic of magnocellular pathways whereas the much more gradual saturation that we observed with disparity vergence is more characteristic of parvocellular pathways: for recent review see Callaway (2005). We suggest that the three short-latency ocular responses provide a promising model system for studying the low-level mechanisms sensing 1st-order motion and disparity, objectively and quantitatively.

Acknowledgements

This research was supported by the Intramural Research Program of the NIH, the National Eye Institute.

References

Adelson EH. Some new motion illusions, and some old ones, analysed in terms of their Fourier components. Investigative Ophthalmology and Visual Science 1982;34(Suppl):144.Abstract

Adelson EH, Bergen JR. Spatiotemporal energy models for the perception of motion. Journal of the Optical Society of America A 1985;2:284–299.

Albrecht DG, Geisler WS, Frazor RA, Crane AM. Visual cortex neurons of monkeys and cats: temporal dynamics of the contrast response function. Journal of Neurophysiology 2002;88:888–913. [PubMed: 12163540]

Albrecht DG, Hamilton DB. Striate cortex of monkey and cat: contrast response function. Journal of Neurophysiology 1982;48:217–237. [PubMed: 7119846]

Baro JA, Levinson E. Apparent motion can be perceived between patterns with dissimilar spatial frequencies. Vision Research 1988;28:1311–1313. [PubMed: 3256148]

Brainard DH. The Psychophysics Toolbox. Spatial Vision 1997;10:433–436. [PubMed: 9176952]

Brown RO, He S. Visual motion of missing-fundamental patterns: motion energy versus feature correspondence. Vision Research 2000;40:2135–2147. [PubMed: 10878275]

Busettini C, Fitzgibbon EJ, Miles FA. Short-latency disparity vergence in humans. Journal of Neurophysiology 2001;85:1129–1152. [PubMed: 11247983]

Busettini C, Masson GS, Miles FA. Radial optic flow induces vergence eye movements with ultra-short latencies. Nature 1997;390:512–515. [PubMed: 9394000]

Busettini C, Miles FA, Krauzlis RJ. Short-latency disparity vergence responses and their dependence on a prior saccadic eye movement. Journal of Neurophysiology 1996;75:1392–1410. [PubMed: 8727386]

Callaway EM. Structure and function of parallel pathways in the primate early visual system. Journal of Physiology 2005;566:13–19. [PubMed: 15905213]

Campbell FW, Howell ER, Robson JG. The appearance of gratings with and without the fundamental Fourier component. Journal of Physiology 1971;217:17P–18P.

Cogan AI, Kontsevich LL, Lomakin AJ, Halpern DL, Blake R. Binocular disparity processing with opposite-contrast stimuli. Perception 1995;24:33–47. [PubMed: 7617417]

Cogan AI, Lomakin AJ, Rossi AF. Depth in anticorrelated stereograms: effects of spatial density and interocular delay. Vision Research 1993;33:1959–1975. [PubMed: 8249313]

Collewijn H, Van Der Mark F, Jansen TC. Precise recording of human eye movements. Vision Research 1975;15:447–450. [PubMed: 1136166]

Cumming BG, DeAngelis GC. The physiology of stereopsis. Annual Review of Neuroscience 2001;24:203–238.

Cumming BG, Parker AJ. Responses of primary visual cortical neurons to binocular disparity without depth perception. Nature 1997;389:280–283. [PubMed: 9305841]

Cumming BG, Shapiro SE, Parker AJ. Disparity detection in anticorrelated stereograms. Perception 1998;27:1367–1377. [PubMed: 10505181]

Edwards M, Pope DR, Schor CM. Orientation tuning of the transient-stereopsis system. Vision Research 1999;39:2717–2727. [PubMed: 10492832]

Edwards M, Pope DR, Schor CM. First- and second-order processing in transient stereopsis. Vision Research 2000;40:2645–2651. [PubMed: 10958914]

Edwards M, Schor CM. Depth aliasing by the transient-stereopsis system. Vision Research 1999;39:4333–4340. [PubMed: 10789427]

Enright JT. Art and the oculomotor system: perspective illustrations evoke vergence changes. Perception 1987a;16:731–746. [PubMed: 3454431]

Enright JT. Perspective vergence: oculomotor responses to line drawings. Vision Research 1987b; 27:1513–1526. [PubMed: 3445485]

Erkelens CJ, Collewijn H. Eye movements and stereopsis during dichoptic viewing of moving random-dot stereograms. Vision Research 1985a;25:1689–1700. [PubMed: 3832593]

Erkelens CJ, Collewijn H. Motion perception during dichoptic viewing of moving random-dot stereograms. Vision Research 1985b;25:583–588. [PubMed: 4060612]

Erkelens CJ, Collewijn H. Control of vergence: gating among disparity inputs by voluntary target selection. Experimental Brain Research 1991;87:671–678.

Fleet DJ, Wagner H, Heeger DJ. Neural encoding of binocular disparity: energy models, position shifts and phase shifts. Vision Research 1996;36:1839–1857. [PubMed: 8759452]

Frisby JP, Mayhew JE. The relationship between apparent depth and disparity in rivalrous-texture stereograms. Perception 1978;7:661–678. [PubMed: 740507]

Gellman RS, Carl JR, Miles FA. Short latency ocular-following responses in man. Visual Neuroscience 1990;5:107–122. [PubMed: 2278939]

Georgeson MA, Harris MG. The temporal range of motion sensing and motion perception. Vision Research 1990;30:615–619. [PubMed: 2339514]

Georgeson MA, Shackleton TM. Monocular motion sensing, binocular motion perception. Vision Research 1989;29:1511–1523. [PubMed: 2635477]

Halpern DL. Stereopsis from motion-defined contours. Vision Research 1991;31:1611–1617. [PubMed: 1949629]

Hays AV, Richmond BJ, Optican LM. A UNIX-based multiple process system for real-time data acquisition and control. WESCON Conference Proceedings 1982;2:1–10.

He S, Macleod DI. Contrast-modulation flicker: dynamics and spatial resolution of the light adaptation process. Vision Research 1998;38:985–1000. [PubMed: 9666981]

Hess RF, Wilcox LM. Linear and non-linear filtering in stereopsis. Vision Research 1994;34:2431–2438. [PubMed: 7975282]

Heuer HW, Britten KH. Contrast dependence of response normalization in area MT of the rhesus macaque. Journal of Neurophysiology 2002;88:3398–3408. [PubMed: 12466456]

Jones R, Kerr KE. Vergence eye movements to pairs of disparity stimuli with shape selection cues. Vision Research 1972;12:1425–1430. [PubMed: 5071112]

Judge SJ. How is binocularity maintained during convergence and divergence? Eye 1996;10(Pt 2):172–176. [PubMed: 8776445]

Kodaka, Y.; Sheliga, BM.; FitzGibbon, EJ.; Miles, FA. Radial-flow vergence eye movements depend critically on the local Fourier components of the motion stimulus [Abstract]; Journal of Vision. 2005. p. 588ahttp://journalofvision.org/585/588/588/, doi: 510.1167/1165.1168.1588

Langley K, Fleet DJ, Hibbard PB. Linear and nonlinear transparencies in binocular vision. Proceedings of the Royal Society of London B 1998;265:1837–1845.

Langley K, Fleet DJ, Hibbard PB. Stereopsis from contrast envelopes. Vision Research 1999;39:2313–2324. [PubMed: 10367053]

Levinson E, Blake R. Stereopsis by harmonic analysis. Vision Research 1979;19:73–78. [PubMed: 419703]

Lu ZL, Sperling G. Three systems for visual motion perception. Current Directions in Psychological Science 1996;5:44–53.

MacLeod DI, He S. Visible flicker from invisible patterns. Nature 1993;361:256–258. [PubMed: 8423852]

MacLeod DI, Williams DR, Makous W. A visual nonlinearity fed by single cones. Vision Research 1992;32:347–363. [PubMed: 1574850]

Masson GS, Busettini C, Miles FA. Vergence eye movements in response to binocular disparity without depth perception. Nature 1997;389:283–286. [PubMed: 9305842]

Masson GS, Busettini C, Yang DS, Miles FA. Short-latency ocular following in humans: sensitivity to binocular disparity. Vision Research 2001;41:3371–3387. [PubMed: 11718780]

Masson GS, Castet E. Parallel motion processing for the initiation of short-latency ocular following in humans. The Journal of Neuroscience 2002;22:5149–5163. [PubMed: 12077210]

Masson GS, Yang DS, Miles FA. Version and vergence eye movements in humans: open-loop dynamics determined by monocular rather than binocular image speed. Vision Research 2002;42:2853–2867. [PubMed: 12450510]

Mayhew JEW, Frisby JP. Psychophysical and computational studies towards a theory of human stereopsis. Artificial Intelligence 1981;17:349–385.

Miles FA. The neural processing of 3-D visual information: evidence from eye movements. The European Journal of Neuroscience 1998;10:811–822. [PubMed: 9753150]

Miles FA, Kawano K, Optican LM. Short-latency ocular following responses of monkey. I. Dependence on temporospatial properties of visual input. Journal of Neurophysiology 1986;56:1321–1354. [PubMed: 3794772]

Mitchell DE. Properties of stimuli eliciting vergence eye movements and stereopsis. Vision Research 1970;10:145–162. [PubMed: 5440779]

Miura K, Matsuura K, Taki M, Tabata H, Inaba N, Kawano K, Miles FA. The visual motion detectors underlying ocular following responses in monkeys. Vision Research 2006;46:869–878. [PubMed: 16356529]

Naka KI, Rushton WA. S-potentials from colour units in the retina of fish (Cyprinidae). Journal of Physiology 1966;185:536–555. [PubMed: 5918058]

Ohzawa I, DeAngelis GC, Freeman RD. Stereoscopic depth discrimination in the visual cortex: neurons ideally suited as disparity detectors. Science 1990;249:1037–1041. [PubMed: 2396096]

Parker AJ, Cumming BG. Cortical mechanisms of binocular stereoscopic vision. Progress in Brain Research 2001;134:205–216. [PubMed: 11702545]

Pelli DG. The VideoToolbox software for visual psychophysics: transforming numbers into movies. Spatial Vision 1997;10:437–442. [PubMed: 9176953]

Pope DR, Edwards M, Schor CM. Orientation and luminance polarity tuning of the transient-vergence system. Vision Research 1999a;39:575–584. [PubMed: 10341986]

Pope DR, Edwards M, Schor CS. Extraction of depth from opposite-contrast stimuli: transient system can, sustained system can't. Vision Research 1999b;39:4010–4017. [PubMed: 10748934]

Prince SJ, Cumming BG, Parker AJ. Range and mechanism of encoding of horizontal disparity in macaque V1. Journal of Neurophysiology 2002;87:209–221. [PubMed: 11784743]

Prince SJ, Pointon AD, Cumming BG, Parker AJ. Quantitative analysis of the responses of V1 neurons to horizontal disparity in dynamic random-dot stereograms. Journal of Neurophysiology 2002;87:191–208. [PubMed: 11784742]

Qian N. Computing stereo disparity and motion with known binocular properties. Neural Computation 1994;6:390–404.

Read JC, Cumming BG. Testing quantitative models of binocular disparity selectivity in primary visual cortex. Journal of Neurophysiology 2003;90:2795–2817. [PubMed: 12867533]

Read JC, Parker AJ, Cumming BG. A simple model accounts for the response of disparity-tuned V1 neurons to anticorrelated images. Visual Neuroscience 2002;19:735–753. [PubMed: 12688669]

Ringach DL, Hawken MJ, Shapley R. Binocular eye movements caused by the perception of three-dimensional structure from motion. Vision Research 1996;36:1479–1492. [PubMed: 8762765]

Robinson DA. A method of measuring eye movement using a scleral search coil in a magnetic field. Institute of Electronic and Electrical Engineers: Transactions in Biomedical Engineering 1963;BME-10:137–145.

Sato M, Edwards M, Schor CM. Envelope size-tuning for transient disparity vergence. Vision Research 2001;41:1695–1707. [PubMed: 11348651]

Schor CM, Edwards M, Sato M. Envelope size tuning for stereo-depth perception of small and large disparities. Vision Research 2001;41:2555–2567. [PubMed: 11520503]

Sclar G, Maunsell JH, Lennie P. Coding of image contrast in central visual pathways of the macaque monkey. Vision Research 1990;30:1–10. [PubMed: 2321355]

Scott-Samuel NE, Georgeson MA. Does early non-linearity account for second-order motion? Vision Research 1999;39:2853–2865. [PubMed: 10492815]

Sheliga BM, Chen KJ, FitzGibbon EJ, Miles FA. Initial ocular following in humans: a response to first-order motion energy. Vision Research 2005a;45:3307–3321. [PubMed: 15894346]

Sheliga BM, Chen KJ, Fitzgibbon EJ, Miles FA. Short-latency disparity vergence in humans: evidence for early spatial filtering. Annals of the New York Academy of Sciences 2005b;1039:252–259. [PubMed: 15826979]

Sheliga BM, Chen KJ, Fitzgibbon EJ, Miles FA. The initial ocular following responses elicited by apparent-motion stimuli: Reversal by inter-stimulus intervals. Vision Research 2006a;46:979–992. [PubMed: 16242168]

Sheliga BM, Kodaka Y, FitzGibbon EJ, Miles FA. Human ocular following initiated by competing image motions: Evidence for a winner-take-all mechanism. Vision Research 2006b;46:2041–2060. [PubMed: 16487988]

Sheliga BM, Miles FA. Perception can influence the vergence responses associated with open-loop gaze shifts in 3D. Journal of Vision 2003;3:654–676. [PubMed: 14765951]

Stevenson SB. Visual processing in disparity vergence control. Annals of the New York Academy of Sciences 2002;956:492–494. [PubMed: 11960849]

Stevenson SB, Lott LA, Yang J. The influence of subject instruction on horizontal and vertical vergence tracking. Vision Research 1997;37:2891–2898. [PubMed: 9415368]

Takemura A, Inoue Y, Kawano K. Visually driven eye movements elicited at ultra-short latency are severely impaired by MST lesions. Annals of the New York Academy of Sciences 2002a;956:456–459. [PubMed: 11960839]

Takemura A, Inoue Y, Kawano K, Quaia C, Miles FA. Single-unit activity in cortical area MST associated with disparity-vergence eye movements: evidence for population coding. Journal of Neurophysiology 2001;85:2245–2266. [PubMed: 11353039]

Takemura A, Kawano K, Quaia C, Miles FA. Population coding in cortical area MST. Annals of the New York Academy of Sciences 2002b;956:284–296. [PubMed: 11960812]

Usui S, Amidror I. Digital low-pass differentiation for biological signal processing. IEEE Transactions on Biomedical Engineering 1982;29:686–693. [PubMed: 6897393]

Westheimer G, Mitchell DE. The sensory stimulus for disjunctive eye movements. Vision Research 1969;9:749–755. [PubMed: 5798742]

Wilcox LM, Hess RF. Is the site of non-linear filtering in stereopsis before or after binocular combination? Vision Research 1996;36:391–399. [PubMed: 8746228]

Yang D, Fitzgibbon EJ, Miles FA. Short-latency vergence eye movements induced by radial optic flow in humans: dependence on ambient vergence level. Journal of Neurophysiology 1999;81:945–949. [PubMed: 10036301]

Yang DS, FitzGibbon EJ, Miles FA. Short-latency disparity-vergence eye movements in humans: sensitivity to simulated orthogonal tropias. Vision Research 2003;43:431–443. [PubMed: 12536000]

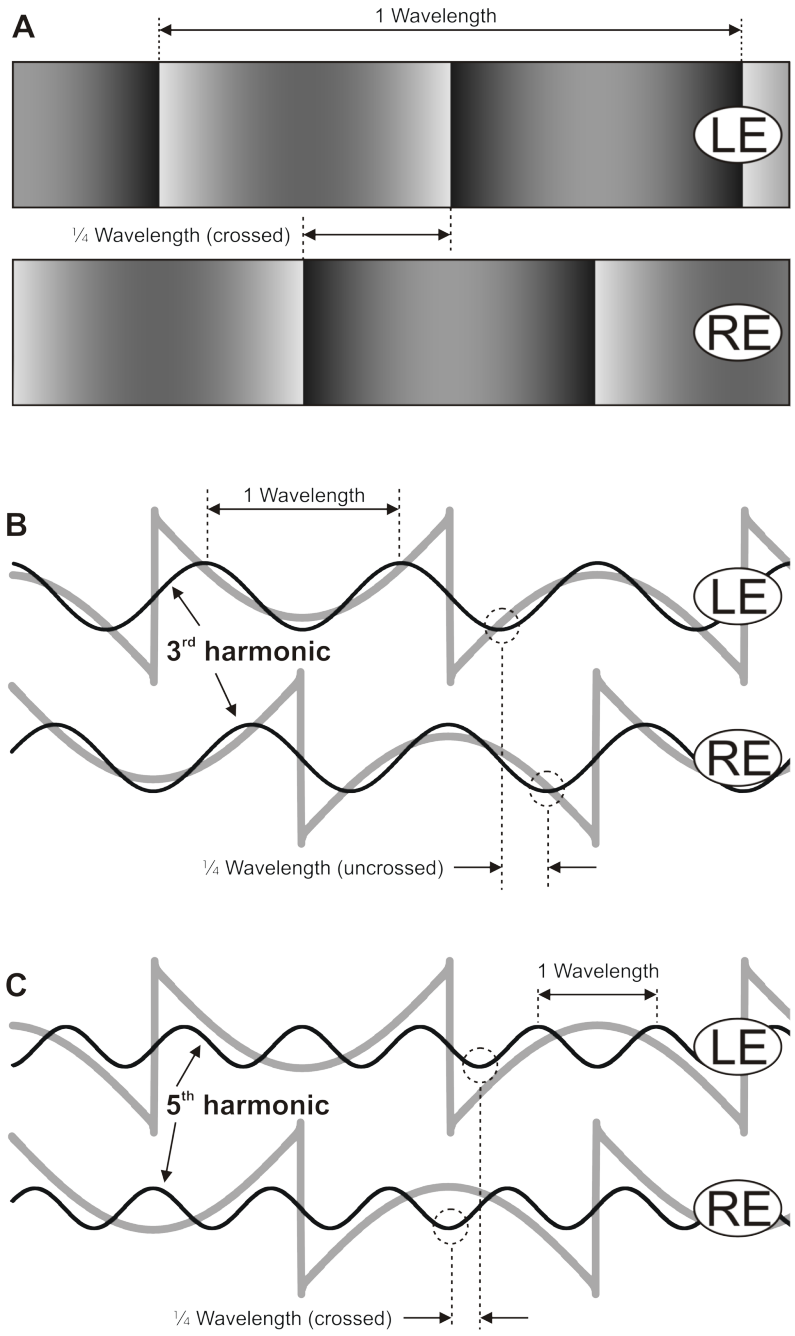

Fig. 1.

The vertical missing fundamental (*mf*) gratings used to explore horizontal disparity vergence. A: *x-y* plot of the luminance, showing the two vertical grating patterns as seen by the left (LE) and right eyes (RE) when presented with a ¼-wavelength phase difference that has crossed disparity. B, C: the luminance profiles of the *mf* stimuli seen in A are shown here in grey line, with the 3rd harmonics (in B) and the 5th harmonics (in C) superimposed in black line. The ¼-wavelength phase differences of the 3rd harmonic (uncrossed disparity) and of the 5th harmonic (crossed disparity) are indicated in dashed line.

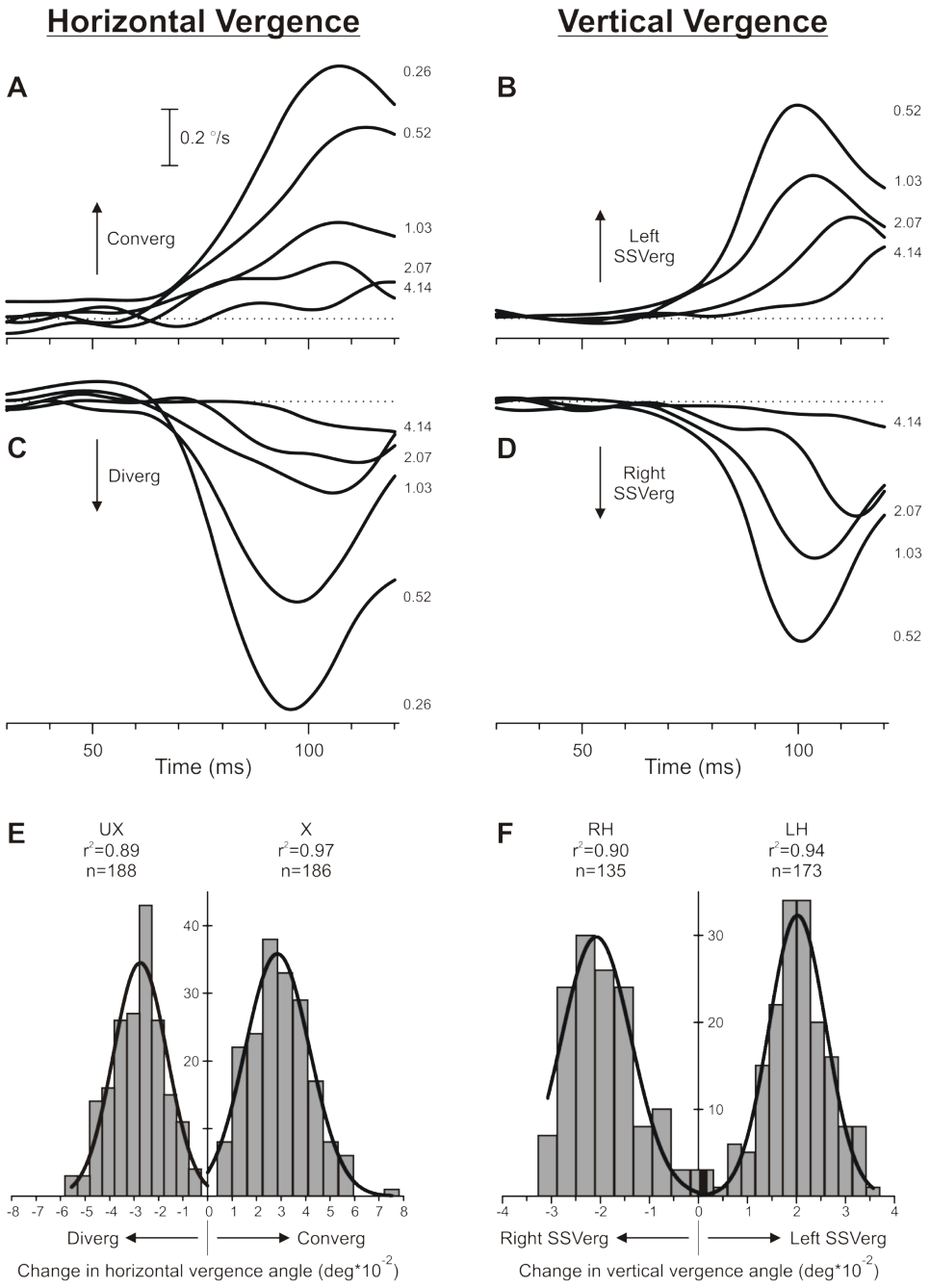

Fig. 2.

The initial vergence responses to ¼-wavelength binocular phase differences applied to pure sine-wave stimuli: dependence on spatial frequency. Upper 2 rows (A–D): Mean vergence velocity profiles (n=131–191) over time—derived from mean position signals by computing the two-point (15 ms apart) central difference between the symmetric weight moving averages (15 points) of the vergence-position sample (Usui & Amidror, 1982)—in response to gratings of various spatial frequencies (indicated in cycles/° by the numbers to the right of the traces, each located at the level of the relevant peak in the profile); horizontal dashed lines, 0°/sec. Bottom row (E, F): Distributions of the measured vergence responses (based on the change in vergence position over the 50-ms time period starting 60 ms after the appearance of the

stimulus) recorded on individual trials in response to a given disparity stimulus: 0.26 cycles/° (E) and 0.52 cycles/° (F); curves are best-fit Gaussian functions (r^2 values and number of measures, n, shown nearby). Left column (A, C, E): Horizontal vergence responses to crossed disparities (A; E, right histogram labeled "X") and uncrossed disparities (C; E, left histogram labeled "UX"); *con*vergent responses have positive sign, indicated by "Converg", and *di*vergent responses have negative sign, indicated by "Diverg". Right column (B, D, F): Vertical vergence responses in response to left-hyper disparities (B; F, right histogram labeled "LH") and right-hyper disparities (D; F, left histogram labeled "RH"); *left* sursumvergent responses have positive sign, indicated by "Left SSVerg", and *right* sursumvergent responses have negative sign, indicated by "Right SSVerg". Contrast, 32%. Subject, NPB.

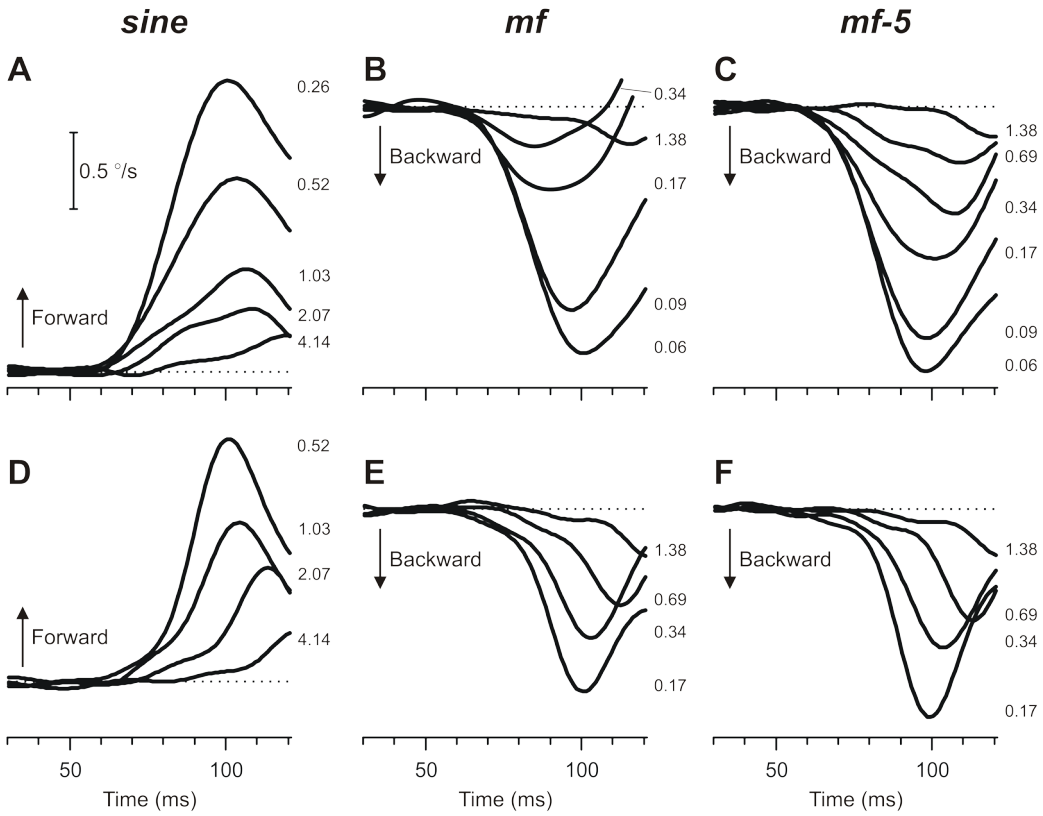

Fig. 3.

The initial vergence responses to ¼-wavelength binocular phase differences applied to various grating patterns: dependence on spatial frequency (mean pooled vergence velocity profiles over time). Top row (A–C): Mean horizontal vergence responses (n=181–191) elicited by horizontal disparities applied to vertical sine-wave stimuli (A), *mf* stimuli (B), and *mf-5* stimuli (C). Bottom row (D–F): Mean vertical vergence responses (n=131–180) elicited by vertical disparities applied to horizontal sine-wave stimuli (D), *mf* stimuli (E), and *mf-5* stimuli (F). Forward responses have positive sign. Spatial frequencies indicated in cycles/° by the numbers to the right of the traces, each located at the level of the relevant peak in the profile. Horizontal dashed lines, 0°/sec. Contrast, 32%. Subject, NPB.

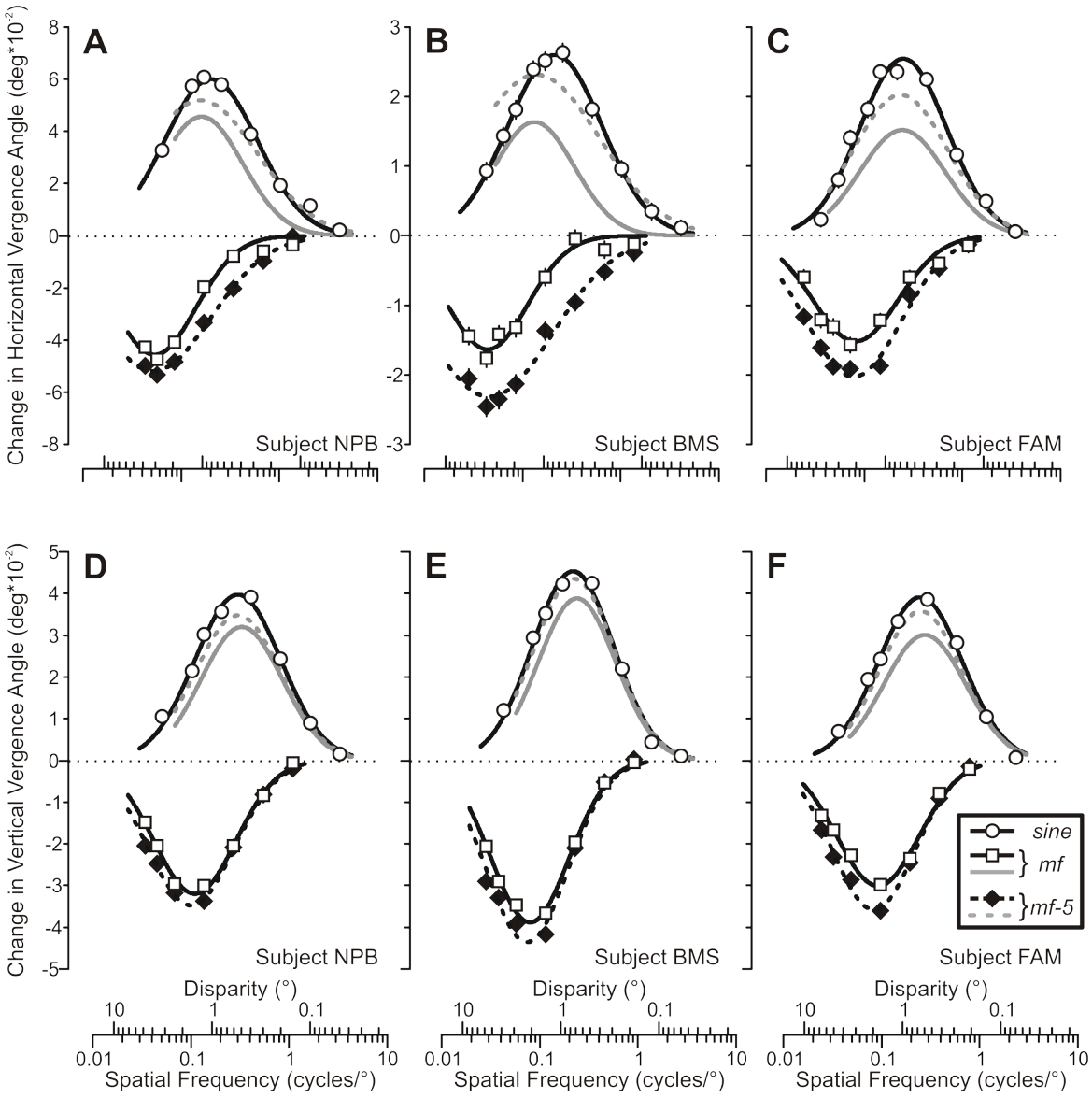

Fig. 4.

The initial vergence responses to ¼-wavelength binocular phase differences applied to various grating patterns: dependence on spatial frequency and disparity (mean pooled vergence position measures for 3 subjects). Top row (A–C): Horizontal vergence responses elicited by horizontal disparities applied to vertical gratings. Bottom row (D–F): Vertical vergence responses elicited by vertical disparities applied to horizontal gratings. Responses to the pure sine-wave stimuli (open circles) were always positive (vergence in the forward direction), whereas those to *mf* (black open squares, black continuous lines) and *mf-5* (black filled diamonds, black dashed lines) stimuli were always negative (vergence in the backward direction). Responses to the *mf* and *mf-5* gratings are also replotted as a function of the spatial frequency (disparity) of their 3rd harmonic to permit easy comparison with the pure sine-wave data (*mf*, grey continuous line; *mf-5*, grey dashed line). A, D: subject NPB (horizontal data: 181–191 trials per condition, SD's ranged 0.013–0.019°; vertical data: 131–180 trials per condition, SD's ranged 0.007–0.010°). B, E: subject BMS (horizontal data: 232–240 trials per condition, SD's ranged 0.017–0.022°; vertical data: 148–159 trials per condition, SD's ranged

0.008–0.013°). C, F: subject FAM (horizontal data: 237–251 trials per condition, SD's ranged 0.012–0.019°; vertical data: 161–177 trials per condition; SD's ranged 0.009–0.013°).

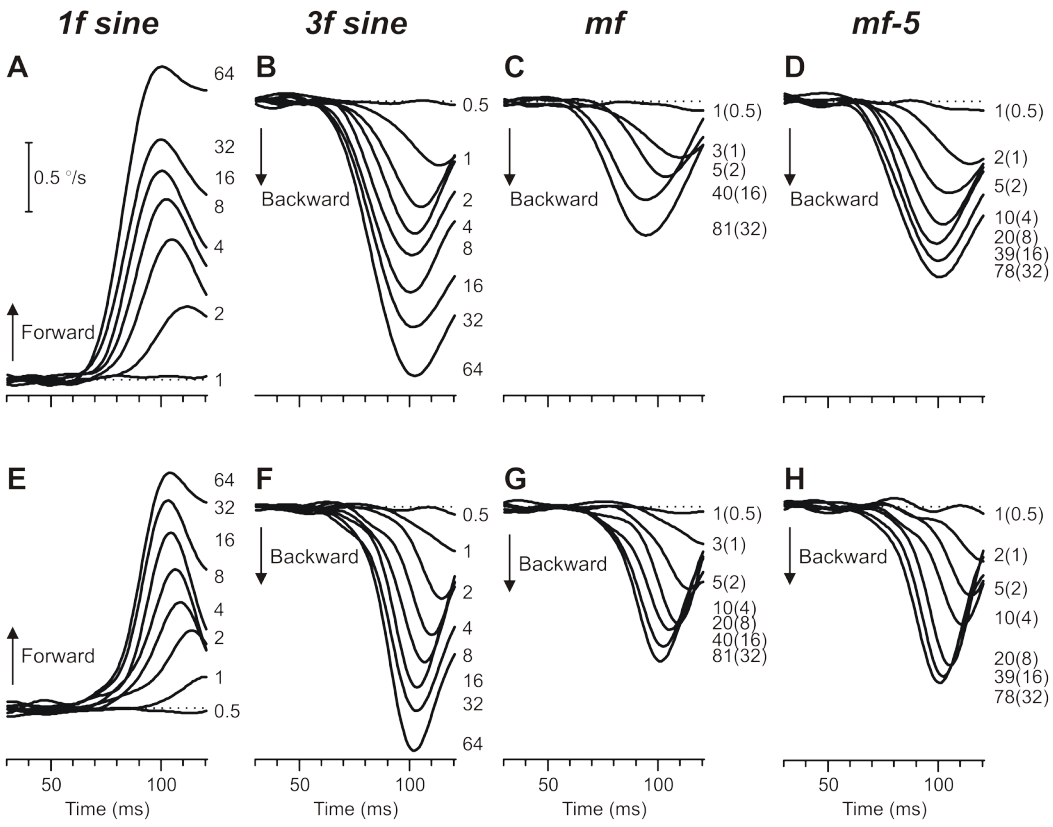

Fig. 5.

The initial vergence responses to ¼-wavelength binocular phase differences applied to various grating patterns: dependence on contrast (mean pooled vergence velocity profiles over time). Top row (A–D): Mean horizontal vergence responses (n=172–182) elicited by horizontal disparities (2.12°) applied to vertical *1f* stimuli (A), *3f* stimuli (B), *mf* stimuli (C), and *mf-5* stimuli (D); spatial frequency of the fundamental, 0.118 cycles/° (wavelength, 8.47°). Bottom row (E–H): Mean vertical vergence responses (n=128–167) elicited by vertical disparities (1.15°) applied to horizontal *1f* stimuli (E), *3f* stimuli (F), *mf* stimuli (G), and *mf-5* stimuli (H); spatial frequency of the fundamental, 0.218 cycles/° (wavelength, 4.59°). Forward responses have positive sign. Contrast indicated by the numbers to the right of the traces, each located at the level of the relevant peak in the profile; for the broadband stimuli, also indicate the contrast of the 3rd harmonic in parentheses. Horizontal dashed lines, 0°/sec. Subject, NPB.

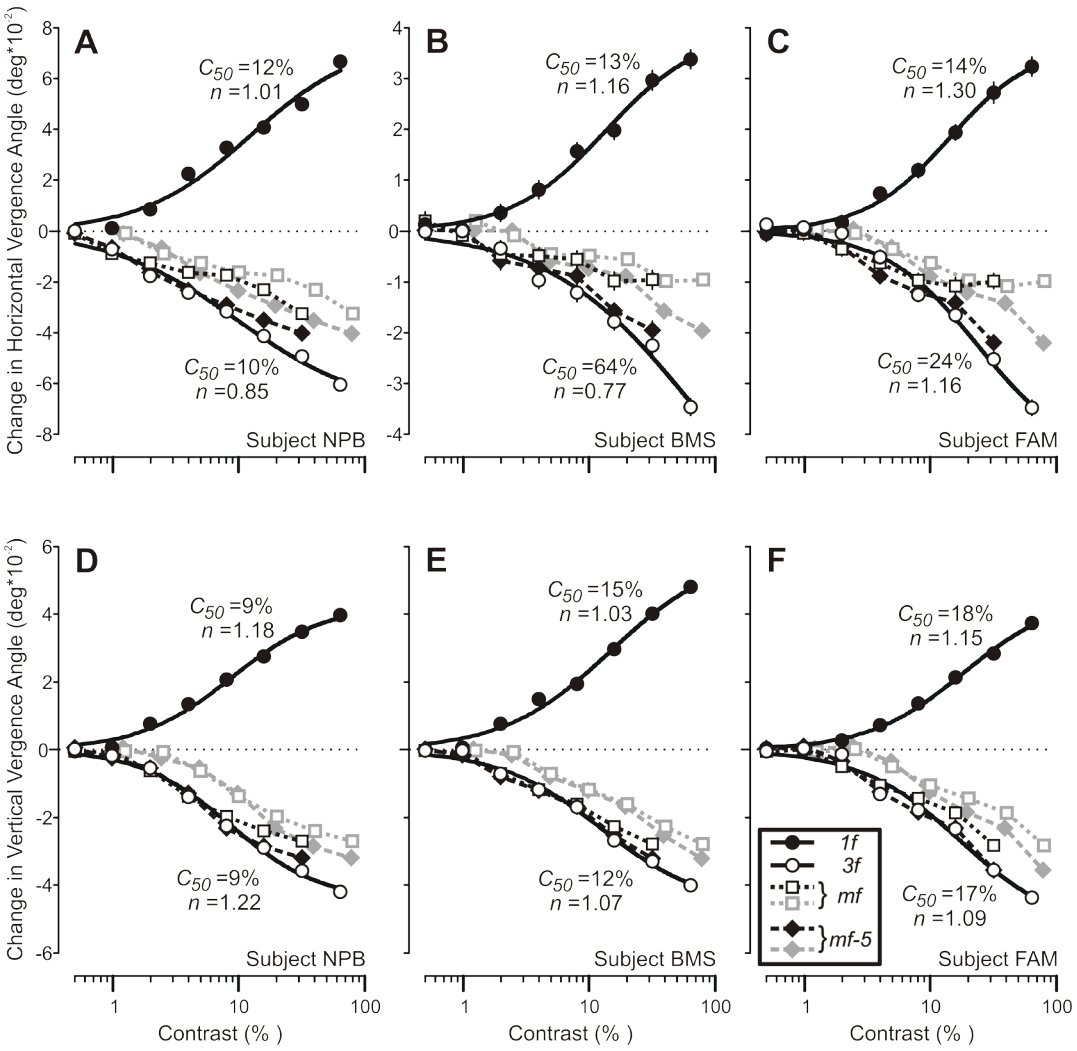

Fig. 6.

The initial vergence responses to ¼-wavelength disparities applied to various grating patterns: dependence on contrast (mean pooled vergence position measures for 3 subjects). Top row (A–C): Horizontal vergence responses elicited by horizontal disparities applied to vertical gratings. Bottom row (D–F): Vertical vergence responses elicited by vertical disparities applied to horizontal gratings. Responses to the pure *1f* stimuli (filled circles) were always positive (vergence in the forward direction), whereas those to *mf* (grey open squares, grey dotted lines), *mf-5* (grey filled diamonds, grey dashed lines), and the pure *3f* (open circles) stimuli were always negative (vergence in the backward direction). Responses to the *mf* and *mf-5* gratings are also plotted as a function of the contrast of their 3rd harmonic to permit easy comparison with the pure *3f* sine-wave data (*mf*, black open squares and dotted line; *mf-5*, black filled diamonds and dashed line). The smooth black curves are best-fit Naka-Rushton functions for the data obtained with the *1f* and *3f* stimuli and the values of their c_{50} and *n* parameters are shown nearby. A, D: subject NPB (horizontal data: 172–182 trials per condition, SD's ranged 0.012–0.018°; vertical data: 128–167 trials per condition, SD's ranged 0.007–0.012°). B, E: subject BMS (horizontal data: 114–120 trials per condition, SD's ranged 0.016–0.021°; vertical data: 127–135 trials per condition, SD's ranged 0.007–0.012°). C, F: subject FAM (horizontal

data: 137–149 trials per condition, SD's ranged 0.014–0.025°; vertical data: 135–140 trials per condition; SD's ranged 0.010–0.015°).

Table 1

Parameters of the best-fit Gaussian functions for the spatial frequency tuning curves in Fig. 4.

		Horizontal			Vertical		
		sine	**mf**	**mf-5**	**sine**	**mf**	**mf-5**
BMS	A_{peak}	0.026	0.016	0.023	0.045	0.039	0.044
	f_0	0.21	0.04 (0.13)	0.05 (0.14)	0.33	0.12 (0.36)	0.11 (0.33)
	σ	0.48	0.41	0.64	0.41	0.40	0.41
	f_{lo}	0.06	0.01 (0.04)	0.01 (0.02)	0.11	0.04 (0.12)	0.04 (0.11)
	f_{hi}	0.79	0.13 (0.40)	0.26 (0.79)	1.00	0.35 (1.05)	0.34 (1.02)
	r^2	0.997	0.970	0.981	0.990	0.996	0.982
FAM	A_{peak}	0.025	0.015	0.020	0.039	0.030	0.036
	f_0	0.25	0.08 (0.24)	0.08 (0.23)	0.37	0.14 (0.41)	0.12 (0.37)
	σ	0.44	0.44	0.48	0.43	0.42	0.42
	f_{lo}	0.07	0.03 (0.08)	0.02 (0.06)	0.12	0.04 (0.13)	0.04 (0.12)
	f_{hi}	0.83	0.27 (0.80)	0.29 (0.87)	1.19	0.43 (1.28)	0.39 (1.17)
	r^2	0.981	0.951	0.982	0.991	0.982	0.990
NPB	A_{peak}	0.060	0.046	0.052	0.040	0.032	0.035
	f_0	0.20	0.05 (0.16)	0.05 (0.16)	0.38	0.14 (0.41)	0.13 (0.38)
	σ	0.47	0.42	0.58	0.44	0.42	0.44
	f_{lo}	0.06	0.02 (0.05)	0.01 (0.03)	0.12	0.04 (0.13)	0.04 (0.12)
	f_{hi}	0.73	0.17 (0.51)	0.25 (0.76)	1.24	0.43 (1.28)	0.41 (1.24)
	r^2	0.987	0.979	0.994	0.992	0.992	0.997

A_{peak}, amplitude of the peak in degrees; f_0, spatial frequency of the peak in cycles/°; σ, standard deviation in log units to the base 10; f_{lo}, f_{hi}, low- and high-frequency cutoff in cycles/°; r^2, coefficient of determination. Values in parentheses are with respect to the 3rd harmonic.